THE JOURNAL OF BIOLOGICAL CHEMISTRY
Vol. 274, No. 9, Issue of February 26, pp. 5746–5754, 1999

Printed in U.S.A.

Calmodulin Mediates Calcium-dependent Activation of the Intermediate Conductance K_{Ca} Channel, *IKCa1**

(Received for publication, October 20, 1998, and in revised form, December 1, 1998)

Christopher M. Fanger‡§, Sanjiv Ghanshani‡§, Naomi J. Logsdon¶§, Heiko Rauer‡, Katalin Kalman‡, Jianming Zhou¶, Kathy Beckingham‖, K. George Chandy‡, Michael D. Cahalan‡, and Jayashree Aiyar¶**

From the ‡Department of Physiology and Biophysics, University of California, Irvine, California 92697, the ¶Target Discovery Department, Zeneca Pharmaceuticals, Wilmington, Delaware 19850, and the ‖Department of Biochemistry and Cell Biology, Rice University, Houston, Texas 77251

Small and intermediate conductance Ca^{2+}-activated K^+ channels play a crucial role in hyperpolarizing the membrane potential of excitable and nonexcitable cells. These channels are exquisitely sensitive to cytoplasmic Ca^{2+}, yet their protein-coding regions do not contain consensus Ca^{2+}-binding motifs. We investigated the involvement of an accessory protein in the Ca^{2+}-dependent gating of *hIKCa1*, a human intermediate conductance channel expressed in peripheral tissues. Calmodulin was found to interact strongly with the cytoplasmic carboxyl (C)-tail of *hIKCa1* in a yeast two-hybrid system. Deletion analyses defined a requirement for the first 62 amino acids of the C-tail, and the binding of calmodulin to this region did not require Ca^{2+}. The C-tail of *hSKCa3*, a human neuronal small conductance channel, also bound calmodulin, whereas that of a voltage-gated K^+ channel, *mKv1.3*, did not. Calmodulin coprecipitated with the channel in cell lines transfected with *hIKCa1*, but not with *mKv1.3*-transfected lines. A mutant calmodulin, defective in Ca^{2+} sensing but retaining binding to the channel, dramatically reduced current amplitudes when co-expressed with *hIKCa1* in mammalian cells. Co-expression with varying amounts of wild-type and mutant calmodulin resulted in a dominant-negative suppression of current, consistent with four calmodulin molecules being associated with the channel. Taken together, our results suggest that Ca^{2+}-calmodulin-induced conformational changes in all four subunits are necessary for the channel to open.

Ca^{2+}-mediated signaling events are central to the physiological activity of diverse cell types. Opening in response to changes in intracellular Ca^{2+} ($[Ca^{2+}]_i$), Ca^{2+}-activated K^+ (K_{Ca})[1] channels play an important role in modulating the Ca^{2+} signaling cascade by regulating the membrane potential in both excitable and nonexcitable cells. Historically, these channels have been classified as large (BK_{Ca}), intermediate (IK_{Ca}), and small (SK_{Ca}) conductance channels based on their single-channel conductance in symmetrical K^+ solutions (1). BK_{Ca} channels have a single channel conductance of 100–250 pS, are opened by elevated $[Ca^{2+}]_i$ as well as by depolarization, and are blocked by the scorpion peptides charybdotoxin (ChTX) and iberiotoxin (2). These channels are abundant in smooth muscle and in neurons and are also present in other cells (2). BK_{Ca} channels are composed of an α- and a β-subunit. The α-subunit, encoded by the *Slo* gene (3–5), is a seven-transmembrane region protein with an extracellular N terminus (6). The β-subunit is a two-transmembrane region protein that, when associated with the channel, enhances the Ca^{2+} sensing and toxin binding properties of the channel (7, 8).

SK_{Ca} channels have unitary conductances of 4–14 pS; are highly sensitive to $[Ca^{2+}]_i$, with activation in the 200–500 nM range; and are voltage-independent (9, 10). SK_{Ca} channels are highly expressed in the central nervous system, where they modulate the firing pattern of neurons via the generation of slow membrane after-hyperpolarizations (10). SK_{Ca} channels have also been described in skeletal muscle (11) and in human Jurkat T-cells (12). These channels are blocked by apamin, a peptide from bee venom, and by the scorpion peptide scyllatoxin (12–14). Three genes (*SKCa1–3*) within a novel subfamily encode SK_{Ca} channels (13). *SKCa1–3* gene products bear 70–80% amino acid sequence identity to each other, and hydrophilicity analysis predicts that these proteins have six transmembrane helices with intracellular N and C termini (13, 15). The *hSKCa3* gene has recently been implicated in schizophrenia (15, 16).

IK_{Ca} channels, unlike SK_{Ca} channels, are predominantly expressed in peripheral tissues, including those of the hematopoietic system, colon, lung, placenta, and pancreas (17–23). These channels have intermediate single channel conductance values of 11–40 pS and can be pharmacologically distinguished from SK_{Ca} channels by their sensitivity to block by ChTX and clotrimazole and by their insensitivity to apamin (20, 22). Both SK_{Ca} and IK_{Ca} channels are voltage-independent and steeply sensitive to a rise in $[Ca^{2+}]_i$. At least one gene encoding an IK_{Ca} channel has been cloned from human and mouse tissues. Called *IKCa1* (also called *KCa4*, *SK4*, and *KCNN4*), this gene has been shown to encode the native IK_{Ca} channel in human T-lymphocytes (22, 23) and erythrocytes (24–27); some patients with Diamond-Blackfan anemia lack one allele of this gene (23). *hIKCa1* shares little sequence identity with the *Slo*

* This study was supported by National Institutes of Health Grants NS14609 and GM41514 (to M. D. C.), GMOD54872 and MH59222 (to K. G. C.), 5T32CA09054 (from NCI) (to C. M. F.), GM49155 and Grant C-1119 from the Welch Foundation (to K. B.), and by a fellowship from the Alexander von Humboldt Foundation (to H. R.). The costs of publication of this article were defrayed in part by the payment of page charges. This article must therefore be hereby marked "*advertisement*" in accordance with 18 U.S.C. Section 1734 solely to indicate this fact.

§ These authors contributed equally to this work.

** To whom correspondence should be addressed: Joan Irvine Smith Hall, Rm. 291, Medical School, University of California, Irvine, CA 92697. Tel.: 949-824-2133; Fax: 949-824-3143; E-mail: gchandy@uci.edu.

[1] The abbreviations used are: K_{Ca}, Ca^{2+}-activated K^+; BK_{Ca}, large conductance K_{Ca}; SK_{Ca} small conductance K_{Ca}; IK_{Ca} intermediate conductance K_{Ca}; C-tail, carboxyl-terminal tail; CAM, calmodulin; ChTX, charybdotoxin; RBL, rat basophilic leukemia; TFP, trifluoperazine; WT, wild-type; GST, glutathione *S*-transferase; PAGE, polyacrylamide gel electrophoresis.

proteins, and only about 40% identity with the *SKCa1–3* gene products. Thus, *hIKCa1* constitutes a distinct subfamily within the extended K^+ channel supergene family.

The Ca^{2+} sensor for BK_{Ca} channels resides in a negatively charged Ca^{2+} bowl domain in the C-tail of the α-subunit (28, 29). The β-subunit also contributes to the gating of these proteins (7). In marked contrast, the protein-coding regions of *SKCa1–3* and *hIKCa1* do not contain any EF-hand or Ca^{2+} bowl motifs in their primary amino acid sequence, despite their exquisite Ca^{2+} sensitivity. This observation led us to speculate that the Ca^{2+} sensor for these channels either resides in a novel motif intrinsic to the channel or is provided by an accessory subunit that is tightly linked to channel activity. We investigated the latter possibility in a yeast two-hybrid system using *hIKCa1* as our prototype. The Ca^{2+}-binding protein calmodulin (CAM) was identified as a strong interacting partner of the C-tail of *hIKCa1*. Recently, CAM was shown to confer Ca^{2+} sensitivity to SK_{Ca} channel subfamily members (30). Here, we report that CAM binds to and is required for Ca^{2+}-dependent activation of *hIKCa1*. Biochemical studies demonstrate that both *hIKCa1* and *hSKCa3* are prebound tightly to CAM in a Ca^{2+}-independent fashion. Finally, we show by expression and patch-clamp recording that four CAMs are required to mediate the Ca^{2+}-dependent channel activity of the *hIKCa1* tetramer.

EXPERIMENTAL PROCEDURES

Clones, Mutants, and Vectors—We have previously reported the cloning of *hIKCa1* (22, 23), *hSKCa3* (15), and *mKv1.3* (31). *Drosophila* wild-type (WT) and mutant (B1234Q) CAMs with differing Ca^{2+} sensitivities have been reported previously (32, 33). The B1234Q mutant has all four EF-hands mutated; glutamates 31, 67, 104, and 140 are replaced by glutamine (33). PAGA2 vector was a kind gift of Lutz Birnbaumer (University of California, Los Angeles, CA). This vector is a pGEM3-based version of the pAGA vector, both of which contain the 5′-untranslated region of alfalfa virus RNA 4 and a 92-base pair poly(A) tail to increase stability of message and for efficient *in vitro* translation. The segments of DNA encoding the C-terminal tails of *hIKCa1* (nucleotides 1252–1678; GenBank™ accession AF022797), *hSKCa3* (nucleotides 1632–2193; GenBank™ accession number AF031815) and *mKv1.3* (nucleotides 1736–2112; GenBank™ accession number M30441) were subcloned into the PAGA2 vector using the polymerase chain reaction with engineered restriction sites. Both CAM clones were also subcloned into the PAGA2 vector. For co-precipitation and electrophysiology experiments (see below), the full-length *hIKCa1* (GenBank™ accession number AF033021) and *mKv1.3* coding regions were fused in-frame with a N-terminal His_6 tag in the pcDNA3.1-His-C vector (Invitrogen, Carlsbad, CA). All clones were verified by sequencing.

Yeast Two-hybrid Screening—A 426-base pair fragment of *hIKCa1* coding for residues 286–427 in the cytoplasmic C-terminal tail of the channel was subcloned into the GAL4 DNA-binding vector (pAS2–1, CLONTECH, Palo Alto, CA) using polymerase chain reaction and engineered restriction sites. This construct was used as bait to screen an activated human leukocyte cDNA library (HL4021AB, CLONTECH). Screening procedures were performed according to the manufacturer's recommendations (CLONTECH PT3061-1). Several thousand putative positives were identified after first-round selection in growth medium; they were then subjected to the colony-lift *lacZ* assay. Positive blue colonies were sequenced using vector-specific primers.

Calmodulin Binding—Two methods were used to test for CAM binding to the channel proteins. The initial deletion constructs of *hIKCa1* were generated by polymerase chain reaction as glutathione *S*-transferase (GST) fusions in the pGEX-6P-1 vector (Amersham Pharmacia Biotech), expressed in the *Escherichia coli* strain *BL21-De3*, and synthesis of the fusion proteins was induced with 0.1 mM isopropyl β-D-thiogalactoside in a liquid culture grown to A_{600} of ~1.0. After 2.5 h at 37 °C, cells were collected by centrifugation, resuspended in NETN lysis buffer (0.5% Nonidet P-40, 1 mM EDTA, 20 mM Tris-HCl (pH 8.0), 100 mM NaCl; 1.0 ml per 20 ml of culture) containing protease inhibitor mixture (complete protease inhibitor mixture tablets, Boehringer Mannheim), and lysed by sonication. The lysate was cleared by centrifugation at 10,000 × *g* for 10 min at 4 °C. GST fusion proteins in the supernatant were adsorbed for 30 min at room temperature to glutathione-Sepharose 4B beads (Amersham Pharmacia Biotech) in NETN (1 volume of lysate:0.4 volume of 50% (v/v) slurry of Sepharose-GSH beads (Amersham Pharmacia Biotech) in NETN), which were then washed with binding buffer containing 1% (v/v) polyoxyethylene-9-lauryl ether, 100 mM NaCl, 20 mM Tris-HCl, pH 8.0. For experiments investigating Ca^{2+} dependence, the above buffer contained, in addition, 1 mM $CaCl_2$ or 2 mM EDTA. Slurries (50% (v/v)) of the bound Sepharose-GSH beads (Sepharose-GSH:GST fusions) were then incubated for 30 min at room temperature in 50 μl of binding buffer containing [^{35}S]methionine-labeled *hCAM*, synthesized by coupled transcription-translation (TnT, Promega, Madison, WI) as described (34). The bound beads were washed three times with binding buffer and resuspended in 15 μl (three volumes) of 2× Laemmli's sample buffer. Proteins released from the beads by boiling in the presence of reducing reagent were analyzed by 4–20% gradient SDS-PAGE followed by autoradiography to detect retention of *hCAM* by the channel-GST fusion proteins. To ensure equivalent protein loading, gels were stained with colloidal blue (Novex, San Diego, CA) to visualize the major protein band in each lane prior to autoradiography. Binding of WT- and B1234Q-CAMs to the C-tail of *hIKCa1* was also determined using the GST pull-down method as above.

For all other experiments, channel constructs in the pAGA2 vector were radiolabeled with [^{35}S]methionine during coupled transcription-translation using reagents from Promega. These constructs were incubated with CAM-Sepharose 4B beads (Amersham Pharmacia Biotech). Briefly, slurries of CAM beads (50% (v/v)) in binding buffer (as described above) were incubated with radiolabeled channel proteins that had been normalized for radioactive incorporation using a PhosphorImager (Molecular Dynamics, Sunnyvale, CA). Equal cpms of each specific protein were added to 50 μl of binding buffer including either 2 mM EDTA or 1 mM Ca^{2+}. Binding and washing conditions were the same as for the GST-Sepharose experiments above. Proteins released from the beads by boiling in the presence of reducing reagent were analyzed by 18% SDS-PAGE followed by autoradiography.

His Tag Pull-down Assays—mKv1.3 and *hIKCa1* expression constructs in pcDNA-3.1His(C) were transfected into COS-7 cells using Fugene6 (Boehringer Manheim) according to the supplied protocol. About 40 h after transfection, 5×10^6 cells were lysed in 10 mM HEPES (pH 7.4), 40 mM KCl, 0.75 mM EDTA (free Ca^{2+} concentration, <1 nM), 1% Triton X-100, 10 mM β-mercaptoethanol, 0.25% deoxycholate, and protease inhibitors. After 20 min on ice, cells were Dounce-homogenized and centrifuged at 2900 × *g* for 15 min to remove insoluble material. The soluble lysate was transferred to a clean tube and mixed with an equal volume of 2× binding buffer (20 mM HEPES (pH 7.4), 200 mM KCl, 20% glycerol, 60 mM imidazole, 20 mM β-mercaptoethanol, and protease inhibitors). The diluted lysate containing the membrane fraction was incubated with Ni^+-NTA resin (Qiagen, Valencia, CA) for ~2 h at 4 °C in order to immobilize the His-tagged channel protein. After extensively washing the resin with wash buffer (10 mM HEPES (pH 7.4), 100 mM KCl, 10% glycerol, 0.25% Triton X-100, 30 mM imidazole, 0.2 mM EDTA, 10 mM β-mercaptoethanol, and protease inhibitors), the channel protein was eluted with elution buffer (same as wash buffer but containing 400 mM imidazole). Proteins from the elution fraction, as well as from the flow-through, were separated by SDS-PAGE and transferred to polyvinylidene fluoride membranes. To determine whether CAM was preassociated with *hIKCa1* or *mKv1.3,* a Western blot analysis was performed using an anti-CAM monoclonal antibody (Upstate Biotechnology, Lake Placid, NY).

Preparation of cRNA, Microinjection, and Whole Cell Recording—Rat basophilic leukemia (RBL) cells were maintained in a culture medium of Eagle's minimum essential medium (BIO-Whittaker, San Diego, CA) supplemented with 1 mM L-glutamine (Sigma) and 10% heat-inactivated fetal calf serum (Summit Biotechnology, Fort Collins, CO) and grown in a humidified, 5% CO_2 incubator at 37 °C. Cells were plated to grow nonconfluently on glass 1 day prior to use for cRNA injection and electrophysiological experiments. T-lymphocytes were isolated from human peripheral blood and activated with phytohemagglutinin (DIFCO, Detroit, MI) as described previously (20). Prior to experimentation, cells were plated for 15 min on glass coverslips coated with poly-L-lysine (Sigma). For other experiments, we stably transfected the COS-7 cell line with *hIKCa1;* the biophysical properties of the *hIKCa1* channels in these cells are indistinguishable from those of IK_{Ca} channels in T-cells (data not shown). Plasmids containing the entire coding sequence of the *hIKCa1* gene, WT-CAM, and B1234Q-CAM were linearized with *Not*I and *in vitro* transcribed with the T7 mMessage mMachine system (Ambion, Austin TX). Plasmids containing the *mKv1.3* coding sequence were linearized with *Eco*RI and *in vitro* transcribed with the Sp6 version of the same kit. The resulting cRNA was phenol/chloroform-purified and stored at −75 °C. RNA concentrations were determined to

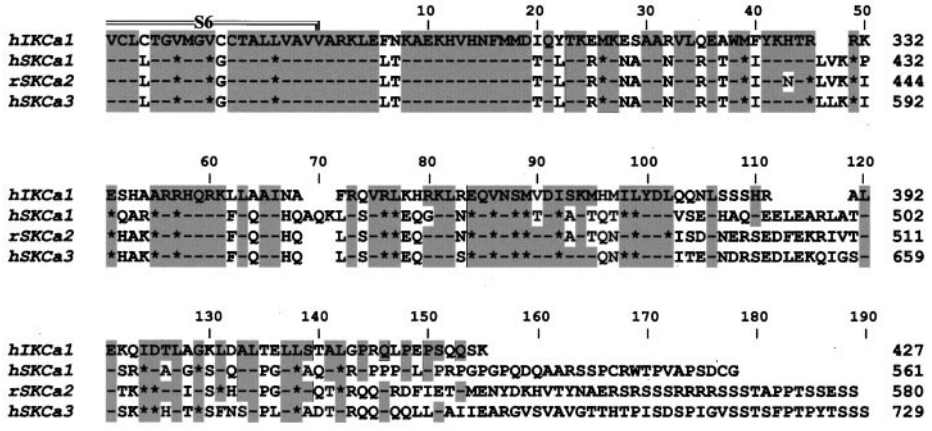

FIG. 1. **Amino acid alignment of the C-terminal tails of *hIKCa1, rSKCa2, hSKCa3,* and *hSKCa1.*** *Dashes* represent identical residues, and *asterisks* correspond to conserved residues. *Shaded areas* represent identical or conserved residues. Numbering shown *above* the sequence alignment is based on the first amino acid in the C terminus (post-S6), as predicted by Kyte-Doolitle hydropathy plots. The numbers shown at the *right* of each sequence correspond to the actual positions of residues in the channel sequence. The C-tail of *hIKCa1* corresponds to residues 286–427 in the protein; the C-tail of *hSKCa1* corresponds to residues 383–561 (GenBank™ accession U69883); the C-tail of *rSKCa2* corresponds to residues 395–580 (GenBank™ accession number U69882); and the C-tail of *hSKCa3* corresponds to residues 543–731.

an accuracy of 25%, based on intensity of bands in agarose gel electrophoresis. The cRNA was diluted with fluorescein isothiocyanate-dextran (Sigma) (average M_r, 10,000; 0.1% in 100 mM KCl). RBL cells were injected with an Eppendorf (Hamburg, Germany) microinjection system (Micro-manipulator 5171 and Transjector 5246) using injection capillaries (Femtotips®, Eppendorf) filled with the cRNA/fluorescein isothiocyanate solution, as described previously (35). Cells were visualized by fluorescence, and *hIKCa1*-specific currents were measured 4–8 h after injection. Cells measured in the whole cell configuration were normally bathed in normal Ringer solution containing 160 mM NaCl, 4.5 mM KCl, 2 mM $CaCl_2$, 1 mM $MgCl_2$, 10 mM HEPES, 10 mM glucose; adjusted to pH 7.4 with NaOH, with an osmolarity of 290–320 mosM. In K^+ Ringer solution, Na^+ was replaced by K^+. A simple syringe-driven perfusion system was used to exchange the bath solutions in the recording chamber. The internal pipette solution with 1 μM free Ca^{2+} contained 145 mM K^+ aspartate, 8.5 mM $CaCl_2$, 2 mM $MgCl_2$, 10 mM HEPES, 10 mM K_2 EGTA; adjusted to pH 7.2 with KOH, with an osmolarity of 290–310 mosM. EGTA was omitted in the high Ca^{2+} internal solution containing 1 mM $CaCl_2$. Pipettes were pulled from glass capillaries, coated with Sylgard (Dow-Corning, Midland, MI), and fire-polished to resistances measured in the bath of 2–5 MΩ. Membrane currents were recorded with an EPC-9 patch-clamp amplifier (HEKA elektronik, Lambrecht, Germany) interfaced to a computer running acquisition and analysis software (Pulse and PulseFit; HEKA elektronik). Data were filtered at 1.5 kHz, and all voltages were corrected for a liquid junction potential offset of −13 mV for aspartate-based solutions. The holding potential in all experiments was −80 mV. For characterization of the *hIKCa1* current, voltage ramp stimuli were used to assess channel activation by elevated $[Ca^{2+}]_i$. RBL cells express an endogenous inwardly rectifying K^+ channel that did not interfere with K_{Ca} currents seen at depolarized potentials. Experiments were performed at room temperature (21–25 °C). The CAM antagonists W7, trifluoperazine (TFP), and calmidazolium were purchased from Calbiochem (La Jolla, CA). ChTX was obtained either from Peptides International, (Louisville, KY) or from BACHEM Biosciences (King of Prussia, PA). Clotrimazole was purchased from Sigma. All slope conductances reported in the text are written as mean ± S.E. (number of cells or experiments).

RESULTS

CAM Binds the C-tail of hIKCa1 in a Ca^{2+}-independent Manner—We searched for accessory molecules that bind to *hIKCa1* using the yeast two-hybrid system. We reasoned that if such a molecule is involved in Ca^{2+} sensing, it must be common to IK_{Ca} and SK_{Ca} channels, because their Ca^{2+} sensitivities and gating behavior are remarkably similar (10, 13, 20, 22, 24). An amino acid alignment of *hIKCa1* with *hSKCa1, rSKCa2,* and *hSKCa3* revealed that except for the pore and the transmembrane regions, the proximal half of the cytoplasmic C-tail was the most highly conserved (Fig. 1); the C-tail of *hIKCa1* was therefore employed as the bait. We chose an activated human leukocyte cDNA library to screen for interaction partners because *hIKCa1* has been previously shown to be highly up-regulated in activated lymphocytes (20, 22). A primary screen using the triple nutrient selection ($Trp^+Leu^+His^+$) resulted in the identification of several thousand positive clones. A subsequent subscreen of 500 colonies yielded nine clones that were positive for β-galactosidase activity. Seven of these clones encoded *CAM*.

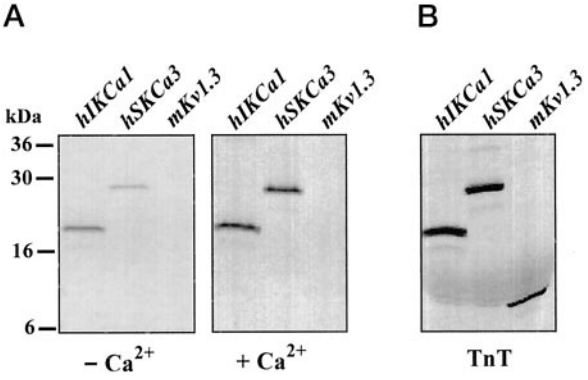

FIG. 2. **CAM binds to the C-tail of *hIKCa1* and *hSKCa3,* but not *mKv1.3.*** *A,* ^{35}S-labeled C-tails of *hIKCa1*, *hSKCa3,* and *mKv1.3* were incubated with CAM-Sepharose beads in the presence (*right panel*) and in the absence (*left panel*) of 1 mM Ca^{2+}, washed, boiled, and loaded on SDS-PAGE gels. Bands were visualized by autoradiography. A faint nonspecific band seen in the *mKv1.3* lane in the presence of Ca^{2+} was also detected when the fragment was incubated with GST-Sepharose beads alone (data not shown). *B,* an autoradiogram of ^{35}S-labeled products, synthesized by coupled transcription translation (TnT) and loaded prior to incubation with CAM produced equivalent band intensities in all three lanes.

We next examined the ability of ^{35}S-labeled *in vitro* translated *hIKCa1*-C-tail to bind CAM-Sepharose as assessed by running the product on an SDS-PAGE gel followed by autoradiography. As shown in Fig. 2*A*, a radiolabeled band of ~28 kDa is visible (*hIKCa1*) consistent with the size of the *hIKCa1* C-tail (Fig. 2*B*), indicating that *hIKCa1* and CAM interact. CAM also binds to the C-tail of the SK_{Ca} channel, *hSKCa3* (Fig. 2*A*, ~22-kDa band (*hSKCa3*)), but not the C-tail of the voltage-gated K^+ channel, *mKv1.3* (Fig 2*A*, *mKv1.3*). As an additional specificity control, we performed GST pull-down experiments; CAM did not bind GST alone but interacted with the GST-*hIKCa1* C-tail (Fig. 3*A*). Thus, CAM interacts specifically with members of the IK_{Ca} and SK_{Ca} family.

Surprisingly, the C-tail fragments of *hIKCa1* and *hSKCa3* bound CAM efficiently in buffers containing 2 mM EDTA and no added Ca^{2+} (Fig. 2*A, hIKCa1* and *mKv1.3, right panel*). Deletion analysis revealed that the shorter 1–98 and 1–62 fragments of the *hIKCa1* C-tail also bound CAM efficiently in Ca^{2+}-free conditions (Fig. 3*A, bottom panel;* Fig. 3*B, right panel*). Four additional deletion fragments (45–98, 37–77,

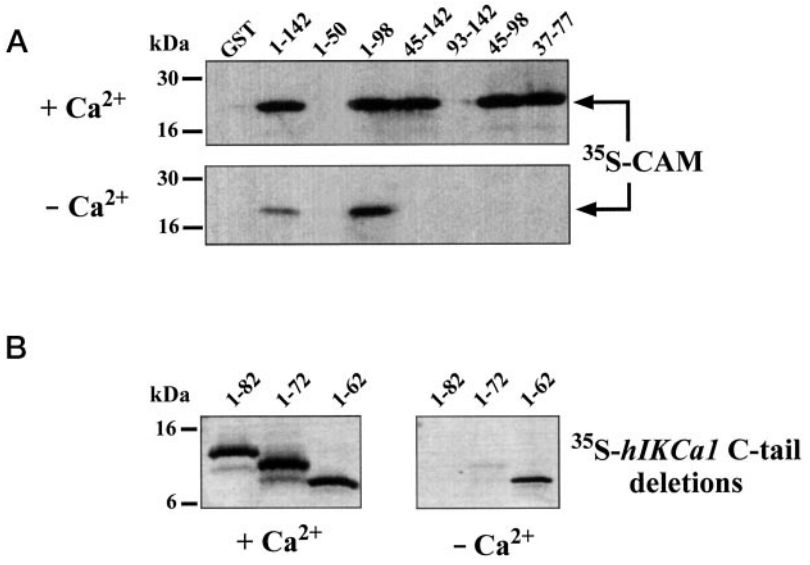

FIG. 3. **Deletion analysis of *hIKCa1* C-tail.** *A,* glutathione-Sepharose beads containing GST fusion constructs of either the entire C-tail or deletion fragments of *hIKCa1* C-tail were incubated with ^{35}S-labeled CAM in the presence of 1 mM Ca^{2+} (*top panel*) or in the presence of 2 mM EDTA and no added Ca^{2+} (*bottom panel*). Coomassie gels ensured equivalent loading of protein in all lanes (data not shown). *B,* deletion constructs 1–82, 1–72, and 1–62 were ^{35}S-labeled by transcription-translation and incubated with CAM-Sepharose beads in the presence of 1 mM Ca^{2+} (*left panel*) or in buffers containing 2 mM EDTA and no added Ca^{2+} (*right panel*).

1–72, and 1–82) bound CAM, but only in the presence of 1 mM Ca^{2+} (Fig. 3*A, top panel;* Fig. 3*B, left panel*), whereas two others (1–50 and 93–142) did not bind CAM at all (Fig. 3). Thus, CAM interacts with the C-tails of *hIKCa1* and *hSKCa3* in the absence of Ca^{2+}, and this property resides in a domain within the first 62 residues of the *hIKCa1* C-tail. The segment between residues 62 and 82 appears to mask the Ca^{2+}-independent interaction of CAM with *hIKCa1*, because the 1–72 and 1–82 fragments bind CAM only in the presence of Ca^{2+}, whereas residues 82–98 appear to reverse the negative effect of 62–82. Removal of as yet unidentified motifs between residues 1 and 37 appears to unmask a Ca^{2+}-dependent interaction with CAM. Interestingly, the 1–98 segment of the *hIKCa1*-C-tail, which contains the Ca^{2+}-independent and Ca^{2+}-dependent modulatory domains, shares a high degree of sequence similarity with the three members of the SK_{Ca} family (Fig. 1).

CAM Co-precipitates with Full-length hIKCa1 in Transfected Cells—The binding data described above suggest that CAM is preassociated with the channel in cells with resting low $[Ca^{2+}]_i$. If this were the case, it should be possible to co-precipitate CAM from cells expressing *hIKCa1*. To test this hypothesis, we expressed an N-terminal His-tagged fusion protein of *hIKCa1* in COS-7 cells, prepared a crude membrane lysate in a Ca^{2+}-free solution, and passed the lysate through a nickel chelate column to allow the *hIKCa1* channel to bind to the column via a His-nickel interaction. The column was washed extensively, and the unbound fraction was collected in the flow-through. The His-tagged *hIKCa1* channel (along with any prebound accessory proteins) was then eluted with 400 mM imidazole. We examined the flow-through and the *hIKCa1*-containing eluate fraction for CAM using a anti-CAM monoclonal antibody. As negative controls, we used membrane lysates from untransfected cells and lysates from cells expressing a His-tagged version of the *mKv1.3* channel that does not bind CAM (Fig. 2*A*). As expected for a ubiquitous protein expressed at high levels in mammalian cells, CAM was detected in the flow-though fractions from untransfected cells (Fig. 4), *mKv1.3*-transfected cells, and *hIKCa4*-transfected cells. In contrast, CAM was detected only in the *hIKCa1*-containing eluate, but not in the eluates from untransfected or *mKv1.3*-transfected cells (Fig. 4). Thus, CAM specifically co-precipitates with full-length *hIKCa1*, but not *mKv1.3*, suggesting that the IK_{Ca} channel is tightly bound to CAM under basal conditions in mammalian cells.

CAM Antagonists Do Not Alter K_{Ca} Channel Function—In T lymphocytes or in mammalian cells expressing *hIKCa1*, elevating $[Ca^{2+}]_i$ rapidly opens IK_{Ca} channels, revealing a voltage-independent K^+ current with a reversal potential near −80 mV (20, 22). To investigate the role of CAM in the function of IK_{Ca} channels encoded by *hIKCa1*, we tested whether CAM antagonists might disrupt K_{Ca} currents activated by dialysis of human T cells with a pipette solution containing 1 μM $[Ca^{2+}]_i$. Whole cell recordings revealed two components of K^+ current, an immediately active voltage-gated K^+ current encoded by *hKv1.3*, along with a rapidly activating IK_{Ca} current (Fig. 5*A*, *traces 1* and *2*), as reported previously (20). The time course of the slope conductance of this IK_{Ca} current is shown in Fig. 5*B*. Treatment with the CAM antagonist W7 (10 μM) had no effect on the IK_{Ca} current at physiological potentials. Although it blocked both currents at depolarized potentials (Fig. 5*A*), this suppression is voltage-dependent and is thought to be mediated by a direct effect on the channel, rather than via CAM modulation (36). Another CAM antagonist, TFP (10 μM), also had no effect on IK_{Ca} currents when applied acutely; the slope conductance ratio, pre-TFP/post-TFP was 1.3 ± 0.2 in six cells. Intact cells were also pretreated with TFP, W7, or 2 μM calmidazolium for 15–30 min prior to recording, with no effect (not shown). Inclusion of 10 μM W7 inside the patch pipette in combination with such pretreatment also had no effect; the slope conductance ratio in seven drug-treated cells relative to untreated cells was 1.3 ± 0.3. Similar results were observed in COS-7 cells stably transfected with *hIKCa1*. We conclude that

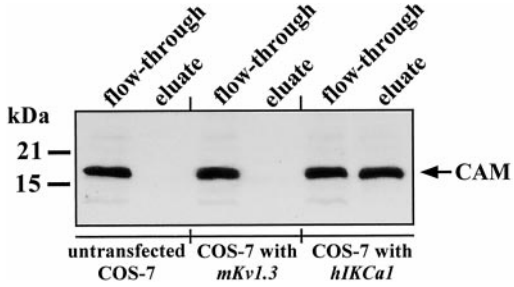

FIG. 4. **CAM co-precipitates with *hIKCa1* in transfected cells.** Lysates from untransfected COS-7 cells or lysates from COS-7 transfected with either N-terminal His-tagged *mKv1.3* or N-terminal His-tagged *hIKCa1,* as indicated, were passed through a nickel-chelate column. The flow-though (unbound fraction) and eluate (channel + prebound accessory proteins) fractions were analyzed for CAM by Western blotting using anti-CAM antibodies.

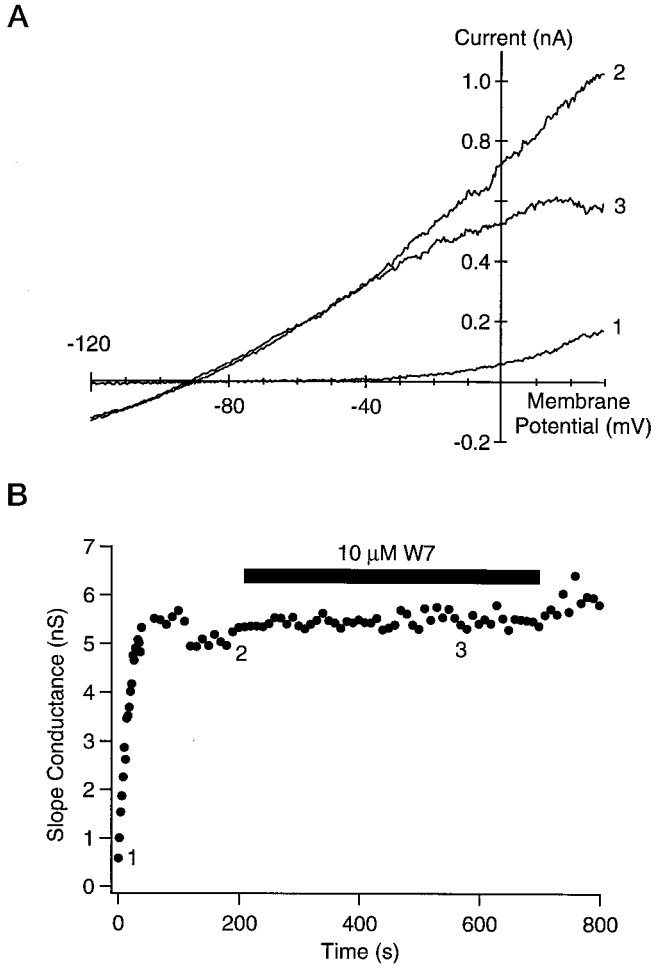

FIG. 5. **CAM antagonists do not inhibit *hIKCa1*.** *A*, currents in activated T-cells were elicited by voltage ramps from −120 to 30 mV over 200 ms. At hyperpolarizing potentials, where only IK_{Ca} currents are observed, acute application of 10 μM W7 to the bath solution had no effect, whereas at depolarized potentials, the current was inhibited. *Numbers* on traces correspond to time of ramp (shown in *B*), where ramp 1 was taken immediately after break-in, ramp 2 at steady-state *hIKCa1* current, and ramp 3 after ~6 min of exposure to 10 μM W7. *B,* time course of *hIKCa1* slope conductance activated by dialysis with 1 μM free Ca^{2+}, determined at −80 mV. After complete and stable activation of *hIKCa1* currents, 10 μM W7 was applied to the bath solution (indicated by the *bar*), but no effect on the K_{Ca} current was observed. Ratio of mean slope conductance of K_{Ca} 2 min after treatment relative to the same cell prior to treatment, 0.9 ± 0.2 (six cells); same ratio for K_V + K_{Ca} current at +25 mV, 0.76 ± 0.02 (six cells)

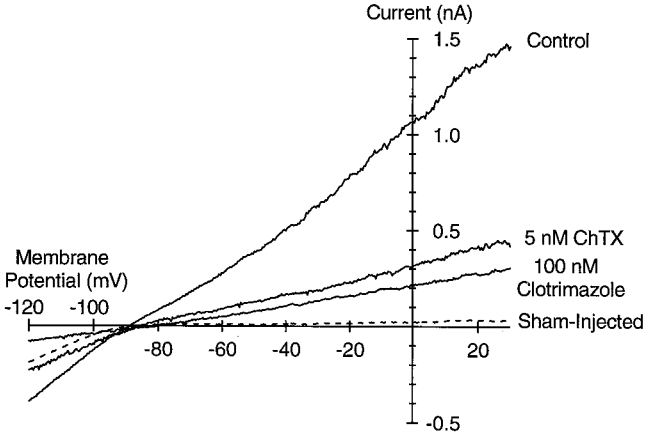

FIG. 6. **Microinjection of *hIKCa1* into RBL cells.** Characterization of currents after injection of FITC only (*dashed line*) or FITC + *hIKCa1* cRNA into RBL cells; typical *hIKCa1* currents were detected 4–7 h postinjection. Currents were elicited by 200-ms voltage ramps, using an internal solution with 1 μM free Ca^{2+}. Application of 5 nM ChTX and 100 nM clotrimazole blocked the IK_{Ca} conductance.

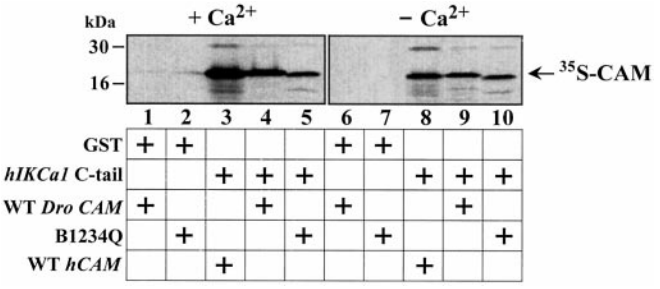

FIG. 7. **Wild-type *Drosophila* CAM and a mutant CAM, B1234Q, interact with the C-tail of *hIKCa1*.** Glutathione-Sepharose beads containing the GST fusion construct of the *hIKCa1* C-tail were incubated with ^{35}S-labeled mammalian WT-CAM, *Drosophila* WT-CAM, or B1234Q-CAM in the presence of 1 mM Ca^{2+} (*left*) or in the presence of 2 mM EDTA and no added Ca^{2+} (*right*).

CAM antagonists do not interfere with the activation of *hIKCa1* channels.

IK_{Ca} Channel Function Requires WT CAM—The association of *hIKCa1* C-tail with CAM in very low [Ca^{2+}] (Figs. 2 and 4), as well as the inability of CAM antagonists to alter current through these channels (Fig. 5), supports the idea of a stable, nonconventional association between CAM and *hIKCa1*. Therefore, to study the interaction of these proteins, simultaneous new synthesis of each might be required. We injected combinations of cRNA encoding channel proteins plus cRNA encoding WT or mutant CAM into RBL cells, enabling us to investigate the effects and interactions of the resulting gene products using electrophysiological techniques. First, we characterized the physiological and pharmacological properties of *hIKCa1* expressed after injection of the encoding cRNA alone. Robust currents exhibiting all the hallmarks of IK_{Ca} channels were seen 4–7 h postinjection (Fig. 6). The currents reversed near −80 mV in normal Ringer solution, and switching the bath solution to K^+-Ringer (164.5 mM K^+) shifted the reversal potential to ~0 mV, as expected from the Nernst equation for a K^+-selective channel (not shown). ChTX or clotrimazole reduced the current in a dose-dependent manner with the expected potency for IK_{Ca} channels in native tissue (20, 22, 24).

To determine whether CAM was responsible for the Ca^{2+}-mediated gating of these channels, we exploited the availability of a *Drosophila* mutant (B1234Q) CAM. *Drosophila* and human CAM are identical at the amino acid level except at five positions. In B1234Q, glutamates (Glu^{31}, Glu^{67}, Glu^{107}, and Glu^{140}) at the −Z coordination positions in each of the four Ca^{2+}-binding sites have been replaced by glutamine, resulting in a dramatically lower affinity for Ca^{2+} (33). We reasoned that co-expressing *hIKCa1* along with B1234Q would result in a significant reduction of current amplitudes. In order for this hypothesis to be tested by co-expression, it was first important to show that B1234Q bound *hIKCa1* normally. The apo form of B1234Q is structurally similar to WT-CAM, the UV CD signal at 222 nm for the B1234Q-apo form being approximately 80% of the wild-type value (33). The apo form of B1234Q would therefore be expected to bind the *hIKCa1* C-tail in a Ca^{2+}-independent fashion. Consistent with this prediction, ^{35}S-labeled *Drosophila* WT- and B1234Q-CAM bound to GST-*hIKCa1* C-tail both in the presence (Fig. 7, *lanes 4* and *5*) and absence (*lanes 9* and *10*) of Ca^{2+}, as did ^{35}S-labeled *hCAM* (*lanes 3* and *8*). These CAMs did not bind GST alone in the presence or absence of Ca^{2+} (Fig. 7, *lanes 1, 2, 6,* and *7*).

Co-injection into RBL cells of WT-CAM cRNA together with

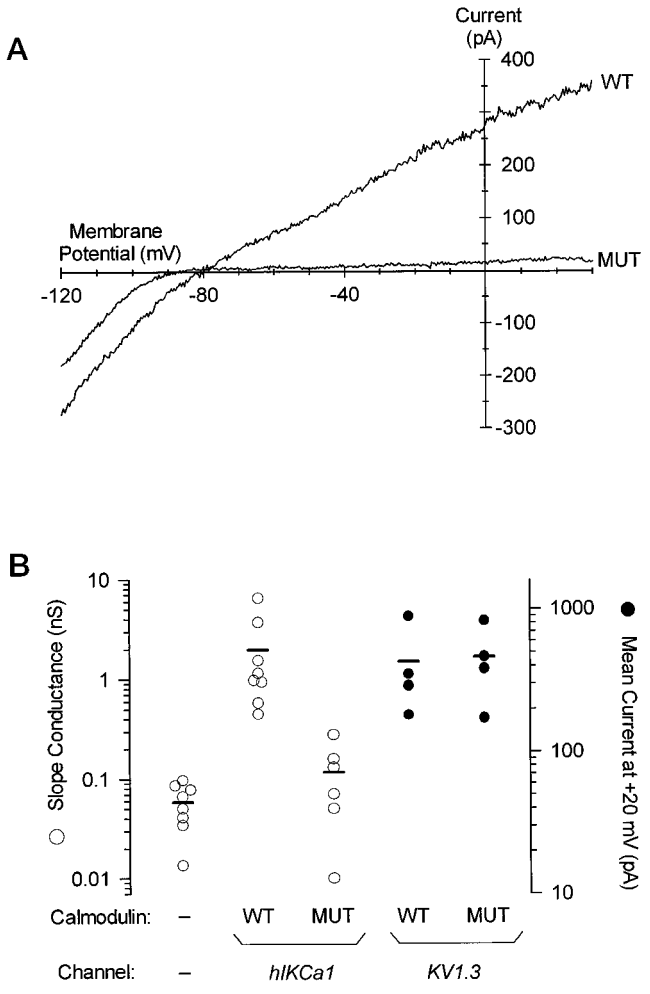

FIG. 8. **Co-injection of *hIKCa1* with mutant CAM inhibits IK_{Ca} currents.** *hIKCa1* cRNA was co-injected into RBL cells with either WT-CAM or B1234Q cRNA. Slope conductance was determined at potentials between –20 and −40 mV to avoid contamination with currents through the endogenous inward-rectifier channel present at potentials below –70 mV. *A,* ramp currents in RBL cells injected with *hIKCa1* in combination with WT-CAM (*WT*) or *hIKCa1* in combination with B1234Q (*MUT*). *B,* comparison of the slope conductance of uninjected cells and those co-injected with *hIKCa1* or KV1.3 and either WT-CAM (*WT*) or B1234Q (*MUT*). Each *circle* represents the measurement of slope conductance of currents in a single cell approximately 2 min after establishing the whole cell mode. The *bold lines* illustrate the mean slope conductance for all cells in each column. The difference between the mean slope conductance of cells microinjected with *B1234Q* RNA and those microinjected with WT-CAM RNA was statistically significant, as illustrated by the one-tailed Student's *t* test ($p < 0.02$). Cells co-injected with *KV1.3* and MUT or WT-CAM showed no significant difference in current at +20 mV.

cRNA encoding the *hIKCa1* channel produced robust *hIKCa1* currents in the whole cell mode with 1 μM free Ca^{2+} in the pipette. In marked contrast, co-injection of B1234Q cRNA with *hIKCa1* cRNA resulted in an average 17-fold reduction in current amplitude. Fig. 8*A* shows the ramp currents obtained from individual cells. Aside from the endogenous inwardly rectifying K^+ current, almost no additional current was seen in the B1234Q-containing cells, as compared with a large outward current observed in the cells with WT-CAM. From experiment to experiment, great variation was noted in the magnitude of currents seen in WT CAM-microinjected cells. However, on a given day, the currents observed in mutant or WT CAM-microinjected cells co-varied in a consistent manner, preserving a statistically significant difference in current ratio. Table I summarizes these results. Overall, injection of mutant CAM reduced currents to 6% of WT CAM-microinjected cells. A reduction in the whole cell K_V current was not observed when B1234Q was coinjected with *mKv1.3* cRNA (mean: 427 pA for WT and 460 pA for B1234Q), ruling out the possibility that the effects on *hIKCa1* currents were due to global inhibition of translation by B1234Q. The results of a typical experiment are shown in Fig. 8*B* and clearly demonstrate that B1234Q inhibits current through *hIKCa1*. B1234Q is incapable of the normal high affinity Ca^{2+} binding and concomitant conformational changes seen in WT-CAM, but it does show a very limited conformational response that is completed upon attaining Ca^{2+} levels of 1 mM (33). However, even with 1 mM Ca^{2+} in the patch pipette, cells expressing B1234Q exhibited no appreciable current (data not shown). Thus, the minimal conformational changes in B1234Q are not adequate to gate the channel, and the normal conformational changes associated with Ca^{2+} binding to CAM are essential for channel opening.

Dominant-negative Suppression of hIKCa1 by B1234Q—Like most K^+ channels, *hIKCa1* is anticipated to be tetrameric, but although each subunit could bind a single CAM, the Ca^{2+} binding requirement for channel activation is unknown. It is conceivable that one functional CAM binding to Ca^{2+} is sufficient to activate an *hIKCa1* channel, or perhaps channel activity requires that all four subunits bind WT CAM and undergo the Ca^{2+}-induced conformational change. To explore this question, we co-injected RBL cells with *hIKCa1* cRNA and a mixture of B1234Q mutant and WT CAM. The mutant and WT CAM composition of *hIKCa1* channels formed in such cells can be predicted by the binomial distribution. The proportion, *P(r)*, of channels with *r* mutant subunits is given by the equation,

$$P(r) = n!/(r!(n-r)!)(p^r(1-p)^{(n-r)}) \quad \text{(Eq. 1)}$$

where *p* is the fraction of mutant CAM in the CAM mix and *n* is the total number of subunits, four in the case of a K^+ channel. The experimental results of microinjecting mutant and WT CAM RNA mixtures can then be compared with these predictions to determine the permitted number of CAM-binding subunits that most accurately represents the observed conductance. Because the mutant CAM appears totally unable to activate *hIKCa1* (Fig. 8), channels with four B1234Q CAMs are presumed to be nonfunctional. Channels containing a mixture of mutant and WT CAM subunits would be expected to conduct only if *hIKCa1* can be activated by fewer than four functional CAM-bound subunits. Thus, the current in cells microinjected with a mixture of mutant and WT CAM should reveal the number of functional CAMs required for active channels. Fig. 9 shows the K_{Ca} current in cells with mixed mutant and WT CAM normalized to control K_{Ca} currents in cells microinjected with WT CAM in parallel experiments performed on the same day. Table I summarizes the results of all experiments. For the case in which even a single mutant subunit will disrupt channel function, the binomial equation simplifies to the equation,

$$P(r) = 4!/(0!(4-0)!)(p^0(1-p)^{(4-0)}) = (1-p)^4 \quad \text{(Eq. 2)}$$

as represented by the solid line (curve 0) in Fig. 9, with *p* plotted as the abscissa. If a single mutant subunit is tolerated in a functional channel, the proportion of conducting channels is shown by the equation,

$$P(r) = 4!/(1!(4-1)!)(p^1(1-p)^{(4-1)}) + (1-p)^4$$
$$= 4(p(1-p)^3) + (1-p)^4 \quad \text{(Eq. 3)}$$

as depicted by Fig. 9, *curve 1*. Similarly expanded equations can be written for cases in which two or three mutant CAM are allowed. The data are well fitted only by the equation in which a single mutant subunit is sufficient to disrupt *hIKCa1* func-

TABLE I

B1234Q mutant CAM suppresses hIKCal currents

RBL cells were measured in whole cell patch-clamp experiments 4–7 h after microinjection with *hIKCal* RNA + CAM RNA. The CAM RNA consisted of wild-type (WT) or B1234Q mutant (MUT) RNA injected separately or together in varying proportions, as indicated. All experiments were performed as a paired comparison between WT and MUT CAM RNA, or WT and the indicated ratio of WT:MUT CAM RNA, using a constant amount of *hIKCal* RNA for each pair. Nine pairs of experiments are shown in the table. Slope conductance values were determined as described in the Fig. 8 legend and are reported in nS as mean ± S.E. (number of cells), with data taken approximately 2 min after establishing the whole cell configuration. Similar ratios of slope conductance were obtained for all experiments employing a given proportion of WT:MUT CAM RNA (see Fig. 9). The day-to-day variations in slope conductance resulted from injections of different amounts of *hIKCal* RNA.

Exp.	WT	All MUT	1 WT:1 MUT	3 WT:1 MUT
	nS	*nS*	*nS*	*nS*
1	1.98 ± 0.74 (8)	0.12 ± 0.04 (6)		
2	15.1 ± 5.0 (10)	1.03 ± 0.24 (6)		
3	22.52 ± 18.5 (6)	1.12 ± 0.23 (4)		
4	38.2 ± 11.6 (5)		2.34 ± 1.19 (6)	
5	5.37 ± 1.25 (6)		0.25 ± 0.07 (11)	
6	22.5 ± 18.5 (6)		1.70 ± 0.68 (5)	
7	22.8 ± 8.4 (10)			13.8 ± 5.3 (10)
8	0.68 ± 0.18 (5)			0.31 ± 0.08 (7)
9	19.4 ± 8.6 (4)			4.4 ± 1.6 (6)

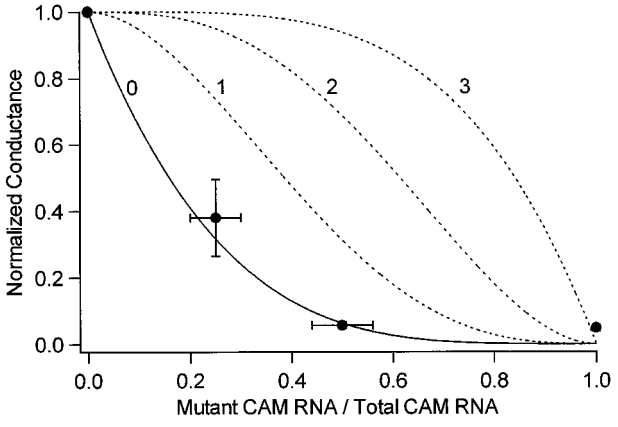

FIG. 9. **Dominant-negative suppression of *hIKCa1* currents by B1234Q.** RBL cells were co-injected with *hIKCa1* cRNA and either WT-CAM alone, B1234Q-CAM alone, or a mixture of *B1234Q*- and WT-CAM cRNA. For each experiment, the base-line conductance (the mean slope conductance of uninjected cells) was subtracted and the resulting number was divided by the mean slope conductance of cells from the same experiment microinjected with WT-CAM. Each *circle* represents the mean ratio ± S.E. of three independent experiments. The ratio of mutant CAM RNA to total CAM RNA is shown on the *x* axis. Each experiment consisted of 4–10 cells measured 4–7 h postinjection. *Error bars* on the *x* axis indicate the maximal anticipated error in RNA concentration. The *solid line* (*line 0*) represents a fit to the binomial distribution for the scenario in which no mutant subunits are allowed in a functional channel. *Dotted lines* (*lines 1–3*) show the fits to the same equation if one, two, or three mutant CAMs, respectively, binding a single *hIKCa1* could form a functional channel.

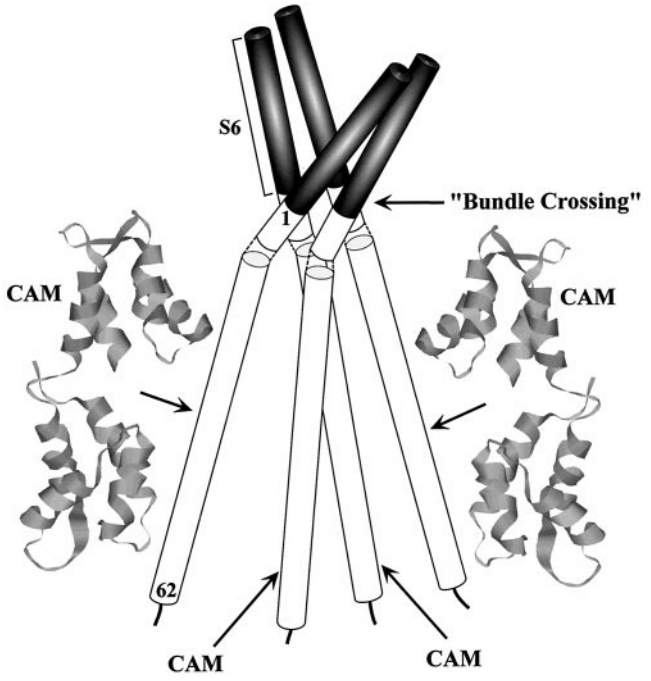

FIG. 10. **Model depicting the site of interaction of CAM with the C-tail.** The inner helices of each channel subunit, shown as *black cylinders,* are arranged in a bundle, as suggested by the KcsA crystal structure (46). These helical rods cross at the bottom cytoplasmic surface (*bundle crossing*) and diverge at the extracellular surface to accommodate the P-regions. The upper end of the helices correspond to the S6 (M2 in KcsA) segments (*black*), and the region below the bundle crossing represents residues 1–10 of the *hIKCa1* C-tail (*white*). Residues 11–62 of the critical C-tail CAM-binding region of each subunit are shown (in scale) as a separate single helix based on both Chou/Fasman and Robson algorithms for secondary structure predictions. Two CAM molecules (actual structure in the absence of Ca^{2+}) are shown in apposition to the C-tail; the other two subunits also associate with CAM. The spatial disposition of the CAMs does not imply interaction with the C-tail in any particular orientation.

tion. Hence, the presence of a B1234Q CAM is dominant-negative for the function of *hIKCa1*.

DISCUSSION

In the present study, we have demonstrated that CAM is prebound to the cytoplasmic C-tail of the intermediate conductance K_{Ca} channel, *hIKCa1,* and mediates Ca^{2+}-dependent gating of these channels. The first 98 amino acids in the C-tail of *hIKCa1* contain subdomains that are critical for both Ca^{2+}-dependent and Ca^{2+}-independent CAM binding. Although this region contains several positively charged and hydrophobic residues reminiscent of CAM-binding sites (37, 38), its lack of dependence on Ca^{2+} for binding is noteworthy. We also show that known CAM antagonists W7 and TFP have no effect on *hIKCa1* current, indicating a novel binding surface for the CAM-*hIKCa1* interaction. Such Ca^{2+}-independent binding of CAM to its target protein, although uncommon, has been reported for some molecules, including nitric oxide synthase, neurogranin, neuromodulin, phosphorylase kinase, and unconventional myosins (39).

Our results with an IK_{Ca} channel parallel and complement those recently reported by Xia *et al.* (30) for SK_{Ca} channels. In that study, CAM was shown to associate tightly with the C-tails of SK_{Ca} channels in the absence of Ca^{2+}. Co-expression in *Xenopus* oocytes of *rSKCa2* and CAM mutants with lower Ca^{2+} binding affinities resulted in a significant decrease in the Ca^{2+} sensitivity of the expressed channel, thus providing the first evidence for a mechanism of Ca^{2+}-gating by SK_{Ca} channels.

Our finding of an identical mechanism for *hIKCa1* expressed in mammalian cells confirms a common mechanism of Ca^{2+} gating for both SK_{Ca} and IK_{Ca} channels, despite their ~40% overall sequence identity. Not surprisingly, the region in the C-tail of *hIKCa1* that we identified as being critical for CAM binding (1–98) shows a high degree of sequence similarity with the corresponding regions in the three members of the SK_{Ca} subfamily of K^+ channels.

In addition to demonstrating that CAM can bind to and mediate the function of *hIKCa1*, we have demonstrated a strong suppression of IK_{Ca} conductance when the channel is co-expressed with a mutant CAM with four defective EF-hand motifs (B1234Q CAM). The fact that the mutant CAM is so effective at competing with the endogenous protein for binding to the channel subunits suggests some mechanism for coassembly of newly synthesized CAM protein with the cytoplasmic tails of new channel molecules as they are folded on the endoplasmic reticulum membranes. Alternatively, it is possible that there is, in essence, no pool of "free" CAM to compete with the newly synthesized protein. At elevated $[Ca^{2+}]_i$, this condition appears to apply, with free (non-target bound) CAM representing about 0.1% of total CAM protein (40). The situation at resting $[Ca^{2+}]_i$ is less well understood. However, studies in muscle cells suggest that the levels of CAM and its target proteins are carefully co-regulated even at resting levels of $[Ca^{2+}]_i$ (41).

If each subunit of *hIKCa1* channel tetramer binds one molecule of Ca^{2+}-free CAM, and if the concerted action of all four molecules is necessary for gating, then perturbing one interaction would impose a dominant-negative phenotype on the channel currents. Consistent with this hypothesis, the currents observed in cells microinjected with a 1:1 ratio of WT and mutant CAM cRNA along with the channel cRNA exhibited about 1/16th of the current magnitude observed in cells microinjected with channel cRNA and WT CAM alone. When the ratio of mutant to WT CAM was varied, we observed that the current relative to WT-CAM-microinjected cells agreed with the equation for disruption of channel activity by binding of a single mutant CAM (Fig. 9). Furthermore, even 1 mM Ca^{2+} in the patch pipette, a concentration sufficient to elicit the conformational changes seen in B1234Q, did not rescue conductance when this mutant CAM was co-expressed with *hIKCa1*. These results imply that Ca^{2+}-induced conformational changes must occur involving each prebound CAM in order to open the channel (Fig. 10). The requirement for four CAM molecules provides a structural basis for the previously determined steeply cooperative Ca^{2+} dependence for activation of the lymphocyte K_{Ca} channel encoded by *hIKCa1* (Hill coefficients of 3–4) (20, 42).

Our results point naturally toward a kinetic model for gating of the IK_{Ca} channel. In the following scheme,

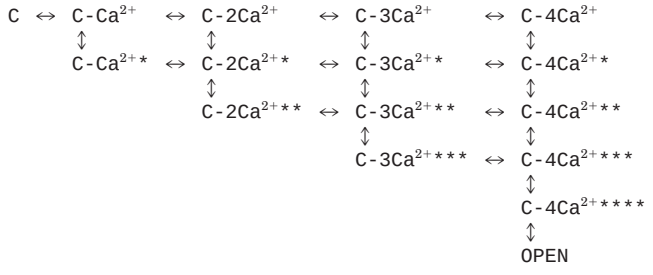

SCHEME 1

C indicates closed channel conformations, and *asterisks* represent activated subunit conformations. Horizontal transitions represent Ca^{2+} binding to CAM on the channel, and vertical transitions represent Ca^{2+}-CAM-induced conformational changes in the channel subunit, with the number of asterisks symbolizing the number of activated subunits. In the above scheme, each subunit of a tetrameric channel is associated with a single CAM, which can bind up to four Ca^{2+} ions to induce a conformational change in the channel subunit. For each of four independent subunits, we envision a sequential two-step activation process: first Ca^{2+} binding by preassociated CAM, and then a conformational change in the IK_{Ca} channel subunit to an activated conformation. In this scheme, it is imagined that conformational changes in the absence of Ca^{2+} binding to CAM are so energetically unfavorable that the states with more activated subunits than Ca^{2+}-CAM moieties do not exist, consistent with the fact that no IK_{Ca} conductance is seen at low $[Ca^{2+}]_i$. Such states, if they existed, would fill in the lower left-hand portion of the scheme. All four subunits must be activated before the channel opens. Although speculative, the kinetic diagram is similar to previous proposals for a variety of K_{Ca} channels based upon single-channel data (43–45). These schemes predict that the steep Hill coefficient determined in functional measurements of the Ca^{2+} sensitivity of channel opening arises from the requirement for Ca^{2+}-induced conformational changes by each of four subunits in BK_{Ca}, SK_{Ca}, and, as proposed here, IK_{Ca} channels.

How might a conformational change in the C-tail of *hIKCa1* result in opening of the pore? A comparison of the sequence of this region with that of the structurally defined bacterial potassium channel, *KcsA*, from *Streptomyces lividans* (46) suggests that the first 6–10 residues of the *hIKCa1* C-tail correspond to part of the inner helix that includes S6 (Fig. 10). More specifically, these residues represent the stretch of the inner helix lying below the "bundle crossing" (Fig. 10), and any Ca^{2+}-CAM-induced conformational change in this segment could conceivably be transmitted along the helical rod, resulting in channel opening. Interestingly, recent studies on the voltage-gated K^+ channel, *Shaker*, suggest that gating occurs at the bundle crossing possibly due to conformational changes in this region (47). Two different algorithms (Chou/Fasman and Robson) predict that the remainder of the 1–62 segment has a high helical propensity, suggesting that the inner helix might extend further cytoplasmically (Fig. 10). Coupling of this segment with the inner helix might underlie calcium gating of *hIKCa1*. This heuristic model requires direct structural verification.

Although second messenger cascades involving CAM are known to modulate many ion channels (48), there is growing evidence of regulation by Ca^{2+}-CAM through direct binding (49). These phenomena have been documented for the *Paramecium* Ca^{2+}-activated sodium channels (50), the *Drosophila* Ca^{2+}-permeable channels *trp* and *trpl* (51, 52), the vertebrate photoreceptors and olfactory receptors involving cyclic nucleotide gated channels (53), the ryanodine receptor Ca^{2+}-release channels (54), and the *N*-methyl-D-aspartate receptors (55). However, the region of the C-tail of *hIKCa1* and *hSKCa3* implicated in Ca^{2+}-free CAM shows no obvious similarity to sequences with a comparable function in *trpl* (51) or the ryanodine receptor (56). In these examples, channel modulation involves either activation or deactivation by CAM. In contrast, the high affinity for Ca^{2+} and the rapid activation kinetics of SK_{Ca} and IK_{Ca} channels demands a fast gating mechanism (45). This "near-intrinsic" requirement is provided by preassociated CAM molecules in a tight multimeric complex with the channel tetramer, converting a modest change in intracellular Ca^{2+} to a quick, robust physiological response. Further biochemical, biophysical, and direct structural studies will help elucidate the mechanisms by which CAM-induced channel conformational changes in the C-tail translate into opening of IK_{Ca}

and SK_{Ca} channels, leading to hyperpolarization and downstream signaling events.

Acknowledgments—We appreciate the expert technical assistance of Luette Forrest and Annabelle Chia-ling Wu, as well as valuable discussions with Drs. George Ehring and George A. Gutman.

REFERENCES

1. Latorre, R., Oberhauser, A., Labarca, P., and Alvarez, O. (1989) *Annu. Rev. Physiol.* **51,** 385–399
2. Kaczorowski, G. J., Knaus, H. G., Leonard, R. J., McManus, O. B., and Garcia, M. L. (1996) *J. Bioenerg. Biomembr.* **28,** 255–267
3. Atkinson, N. S., Robertson, G. A., and Ganetzky, B. (1991) *Science* **253,** 551–555
4. Butler, A., Tsunoda, S., McCobb, D. P., Wei, A., and Salkoff, L. (1993) *Science* **261,** 221–224
5. Tseng-Crank, J., Foster, C. D., Krause, J. D., Mertz, R., Godinot, N., DiChiara, T. J., and Reinhart, P. H. (1994) *Neuron* **13,** 1315–1330
6. Meera, P., Wallner, M., Song, M., and Toro, L. (1997) *Proc. Natl. Acad. Sci. U. S. A.* **94,** 14066–14071
7. Wallner, M., Meera, P., Ottolia, M., Kaczorowski, G. J., Latorre, R., Garcia, M. L., Stefani, E., and Toro, L. (1995) *Recept. Channels* **3,** 185–199
8. Hanner, M., Schmalhofer, W. A., Munujos, P., Knaus, H. G., Kaczorowski, G. J., and Garcia, M. L. (1997) *Proc. Natl. Acad. Sci. U. S. A.* **94,** 2853–2858
9. Hille, B. (1993) *Ionic Channels of Excitable Membranes,* 2nd ed., pp. 121–124, Sinauer, Sunderland, MA
10. Sah, P. (1992) *Trends Neurosci.* **19,** 150–154
11. Vergara, C., and Ramirez, B. U. (1997) *Exp. Neurol.* **146,** 282–285
12. Grissmer, S., Lewis, R. S., and Cahalan, M. D. (1992) *J. Gen. Physiol.* **99,** 63–84
13. Kohler, M., Hirschberg, B., Bond, C. T., Kinzie, J. M., Marrion, N. V., Maylie, J., and Adelman, J. P. (1996) *Science* **273,** 1709–1714
14. Hanselmann, C., and Grissmer, S. (1996) *J. Physiol.* **496,** 627–637
15. Chandy, K. G., Fantino, E., Wittekindt, O., Kalman, K., Tong, L. L., Ho, T. H., Gutman, G. A., Crocq, M. A., Ganguli, R., Nimgaonkar, V., Morris-Rosendahl, D., and Gargus, J. J. (1998) *Mol. Psychiatry* **3,** 32–37
16. Bowen, T., Guy, C. A., Craddock, N., Williams, N., Spurlock, G., Murphy, K., Jones, L., Cardno, A., Gray, M., Sanders, R., McCarthy, M., Chandy, K. G., Fantino, E., Kalman, K., Gutman, G. A., Gargus, J. J., Williams, J., McGuffin, P., Owen, M. J., and O'Donovan, M. C. (1998) *Mol. Psychiatry* **3,** 266–269
17. Gardos, G. (1958) *Biochim. Biophys. Acta* **30,** 653–654
18. Brugnara, C., Armsby, C. C., De Franceschi, L., Crest, M., Euclaire, M. F., and Alper, S. L. (1995) *J. Membr. Biol.* **147,** 71–82
19. Mahaut-Smith, M. P. (1995) *J. Physiol.* **484,** 15–24
20. Grissmer, S., Nguyen, A. N., and Cahalan, M. D. (1993) *J. Gen. Physiol.* **102,** 601–630
21. Gallin, E. K. (1991) *Physiol. Rev.* **71,** 775–811
22. Logsdon, N. J., Kang, J., Togo, J. A., Christian, E. P., and Aiyar, J. (1997) *J. Biol. Chem.* **272,** 32723–32726
23. Ghanshani, S., Coleman, M., Gustavsson, P., Wu, C.-L., Gutman, G. A., Dahl, N., Mohrenweiser, H., and Chandy, K. G. (1998) *Genomics* **51,** 160–161
24. Ishii, T. M., Silvia, C., Hirschberg, B., Bond, C. T., Adelman, J. P., and Maylie, J. (1997) *Proc. Natl. Acad. Sci. U. S. A.* **94,** 11651–11656
25. Joiner, W. J., Wang, L. Y., Tang, M. D., and Kaczmarek, L. K. (1997) *Proc. Natl. Acad. Sci. U. S. A.* **94,** 11013–11018
26. Vandorpe, D. H., Shmukler, B. E., Jiang, L., Lim, B., Maylie, J., Adelman, J. P., de Franceschi, L., Cappellini, M. D., Brugnara, C., and Alper, S. L. (1998) *J. Biol. Chem.* **273,** 21542–21553
27. Jensen, B. S., Strobaek, D., Christophersen, P., Jorgensen, D. T., Hansen, C., Silataroglu, A., Olesen, S.-P., and Ahring, P. K. (1998) *Amer. J. Physiol.* **275,** C848–C856
28. Wei, A., Solaro, C., Lingle, C., and Salkoff, L. (1994) *Neuron* **13,** 671–681
29. Schreiber, M., and Salkoff, L. (1997) *Biophys. J.* **73,** 1355–1363
30. Xia, X.-M., Fakler, B., Rivard, A., Wayman, G., Johnson-Pais, T., Keen, J. E., Ishii, T., Hirschberg, B., Bond, C. T., Lutsenko, S., Maylie, J., and Adelman, J. P. (1998) *Nature* **395,** 503–507
31. Grissmer, S., Dethlefs, B., Wasmuth, J. J., Goldin, A. L., Gutman, G. A., Cahalan, M. D., and Chandy, K. G. (1990) *Proc. Natl. Acad. Sci. U. S. A.* **87,** 9411–9415
32. Maune, J. F., Klee, C. B., and Beckingham, K. (1992) *J. Biol. Chem.* **267,** 5286–5295
33. Mukherjea, P., Maune, J. F., and Beckingham, K. (1996) *Protein Science* **5,** 468–477
34. Pragnell, M., De Waard, M., Mori, Y., Tanabe, T., Snutch, T. P., and Campbell, K. P. (1994) *Nature* **368,** 67–70
35. Ikeda, S. R., Soler, F., Zuhlke, R. D., and Lewis, D. L. (1992) *Pfluegers Arch. Eur. J. Physiol.* **422,** 201–203
36. DeCoursey, T. E., Chandy, K. G., Gupta, S., and Cahalan, M. D. (1985) *J. Neuroimmunol.* **10,** 71–85
37. O'Neil, K. T., and DeGrado, W. F. (1990) *Trends Biochem. Sci.* **15,** 59–64
38. Weinstein, H., and Mehler, E. L. (1994) *Annu. Rev. Physiol.* **56,** 213–236
39. Rhoads, A. R., and Friedberg, F. (1997) *FASEB J.* **11,** 331–340
40. Romoser, V. A., Hinkle, P. M., and Persechini, A. P. (1997) *J. Biol. Chem.* **272,** 13270–13274
41. Bender, P. K., Dedman, J. R., and Emerson, C. P. (1988) *J. Biol. Chem.* **263,** 9733–9737
42. Verheugen, J. A. H. (1998) *J. Physiol.* **508,** 167–177
43. McManus, O. B., and Magleby, K. L. (1991) *J. Physiol.* **443,** 739–777
44. Cox, D. H., Cui, J., and Aldrich, R. W. (1997) *J. Gen. Physiol.* **110,** 257–281
45. Hirschberg, B., Maylie, J., Adelman, J. P., and Marrion, N. V. (1998) *J. Gen. Physiol.* **111,** 565–581
46. Doyle, D. A., Cabral, J. M., Pfuetzner, R. A., Kuo, A., Gulbis, J. M., Cohen, S. L., Chait, B. T., and MacKinnon, R. (1998) *Science* **280,** 69–77
47. Holmgren, M., Shin, K. S., and Yellen, G. (1998) *Neuron* **21,** 617–621
48. Hoger, J. H., Walter, A. E., Vance, D., Yu, L., Lester, H. A., and Davidson, N. (1991) *Neuron* **6,** 227–236
49. Saimi, Y., and Kung, C. (1994) *FEBS Lett.* **350,** 155–158
50. Saimi, Y., and Ling, K. Y. (1990) *Science* **249,** 1441–1444
51. Warr, C. G., and Kelly, L. E. (1996) *Biochem. J.* **314,** 497–503
52. Scott, K., Sun, Y., Beckingham, K., and Zuker, C. S. (1997) *Cell* **91,** 375–383
53. Varnum, M. D., and Zagotta, W. N. (1997) *Science* **278,** 110–113
54. Tripathy, A., Mann, G., and Meissner, G. (1995) *Biophys. J.* **69,** 106–109
55. Zhang, S., Ehlers, M. D., Bernhardt, J. P., Su, C. T., and Huganir, R. L. (1998) *Neuron* **21,** 443–453
56. Guerrini, R., Menegazzi, P., Anacardio, R., Marastoni, M., Tomatis, R., Zorzato, F., and Treves, S. (1995) *Biochemistry* **34,** 5120–5129